Available online at www.sciencedirect.com

ScienceDirect

Mendeleev Commun., 2019, **29**, 102–104

Mendeleev Communications

Effect of post-annealing in air on optical and XPS spectra of Y_2O_3 ceramics doped with CeO_2

Ivan S. Zhidkov,*[a] Roman N. Maksimov,[b,c] Andrey I. Kukharenko,[a] Larisa D. Finkelstein,[d] Seif O. Cholakh,[a] Vladimir V. Osipov[b] and Ernst Z. Kurmaev[a,d]

[a] *Institute of Physics and Technology, Ural Federal University, 620002 Ekaterinburg, Russian Federation. E-mail: i.s.zhidkov@urfu.ru*

[b] *Institute of Electrophysics, Ural Branch of the Russian Academy of Sciences, 620016 Ekaterinburg, Russian Federation*

[c] *SEC 'Nanomaterials and nanotechnologies', Ural Federal University, 620002 Ekaterinburg, Russian Federation*

[d] *M. N. Mikheev Institute of Metal Physics, Ural Branch of the Russian Academy of Sciences, 620108 Ekaterinburg, Russian Federation*

DOI: 10.1016/j.mencom.2019.01.035

Yttrium oxide ceramics doped with CeO_2 (5 mol%) were prepared from nanopowders produced by the laser ablation method. The optical measurements have demonstrated that the transparency of as-sintered ceramic was markedly increased after annealing (T = 1400 °C) under air. XPS data revealed the presence of mixed Ce^{3+} and Ce^{4+} states, while oxygen defect peak decreased after annealing owing to the defect elimination during oxygen diffusion into the highly defective ceramic.

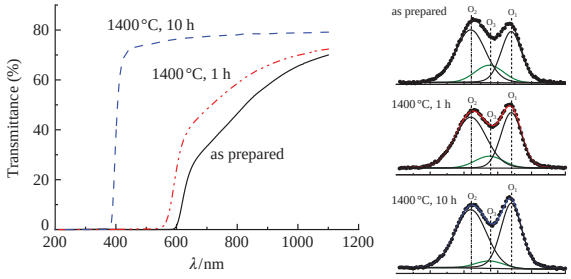

In recent years, yttria became considered as an alternative to traditional laser host materials due primarily to its higher thermal conductivity (13.6 W mK^{-1} for undoped Y_2O_3), lower phonon energies as compared with yttrium–aluminum garnet (YAG), and broad transparent region from UV to IR that can provide the stable laser operations.[1] However, the high melting point and high-temperature phase transition of Y_2O_3 make the growth of single crystal difficult thus seriously restricting the sizes of as-obtained crystals.

On the other hand, transparent polycrystalline ceramics are very difficult to produce since heterogeneities such as pores, grain boundaries, inclusions, *etc*., scatter light in those ceramics.[2,3] Due to the difficulties of removing those heterogeneities in polycrystalline ceramics, most of them are opaque or translucent but still not transparent. It was found that that transparent sintered ceramics should be fabricated from nano-sized particles and should not have pores in the grain boundaries.[4,5] In view of this, special sintering technologies, such as vacuum sintering, vacuum hot pressing, and spark plasma sintering were developed for obtaining fully dense ceramics.

It is known that the transparency reduction in these materials is caused by the presence of oxygen vacancies resulted from the reducing conditions in the vacuum, which give rise to the formation of F and F^+ centers in the wide band gap. These absorption bands can contribute to the transmission performance.[6] The oxygen vacancies in the sintered ceramics can be removed conventionally by post-annealing in air or in an oxygen atmosphere.[7,8] However, the questions of the Ce ions oxidation and influence of oxygen vacancies on the impurity ions still remain important for the optical materials science. In this work, the changes of transparency and filling of oxygen vacancies in Y_2O_3 ceramics doped with CeO_2 (5 mol%) under post-annealing in air[†] were controlled by the direct measurements of optical transmission and X-ray photoelectron spectroscopy (XPS) spectra.

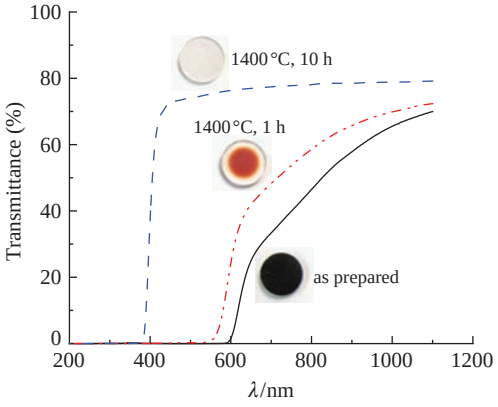

Figure 1 Transmission spectra of as prepared and annealed Y_2O_3 ceramics doped with CeO_2 (5 mol%).

[†] Commercial high-purity powders of Y_2O_3 and CeO_2 (>99%, Lanhit, Russia) were used as raw materials. The powders of Y_2O_3 were dry-mixed with CeO_2 (5 mol%) for 24 h in a rotary mixer with an inclined axis of rotation and size of their nanoparticles was 10–15 nm. The obtained mixture was then compacted at a pressure of 10 MPa and pre-sintered at 1300 °C for 5 h in air for preparation of solid target. To produce the nanopowder, the prepared target was ablated by a radiation from a LAERT pulse-periodical CO_2 laser (λ = 10.6 μm).[9] The obtained nanopowder was compacted into cylindrical green pellets with a diameter of 14 mm and a thickness of 3–4 mm by uniaxial static pressing under a pressure of 200 MPa. Sintering of compacts was carried out at 1780 °C for 20 h

According to the transmission spectra[‡] of as prepared and annealed Y_2O_3 ceramics doped with CeO_2 (5 mol%) (Figure 1), the annealing at 1400 °C improved the transmittance of ceramics, which significantly increased within 10 h.

To explain the nature of observed changes, we evaluated the influence of annealing on the states of oxygen and cerium ions using the XPS method which provides the important information about the valence state and nearest environment of the investigated atoms. XPS survey spectra were measured[§] for the energy range of 1400–0 eV and there were no uncontrolled impurities detected, which evidenced about the high quality of prepared samples.

The measurements of high-energy resolved XPS O 1*s* spectra (Figure 2) revealed the contributions of oxygen atoms in three

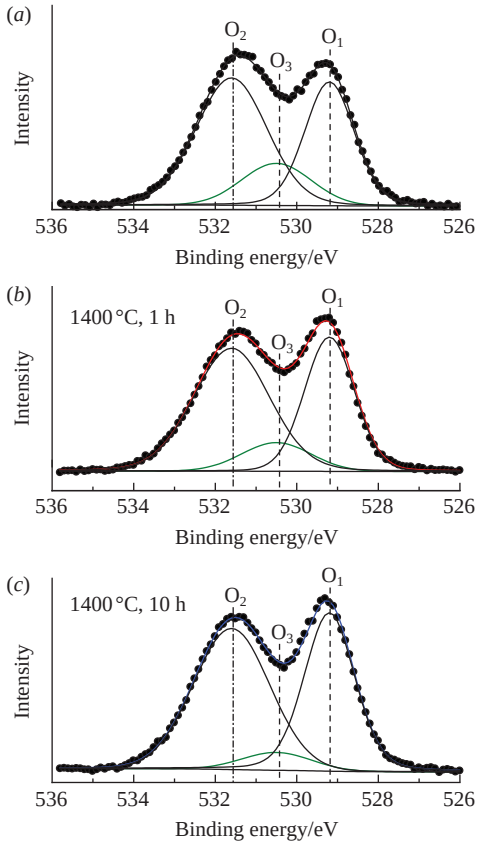

Figure 2 XPS O 1s spectra of (*a*) as prepared and (*b*),(*c*) annealed Y_2O_3 ceramics doped with CeO_2 (5 mol%).

under a residual gas pressure of 10^{-3} Pa. After sintering, some samples were annealed in air at 1400 °C for 1 or 10 h, followed by polishing the surfaces to obtain a mirror gloss using diamond pastes of different granularity.

[‡] The transmission spectra of ceramics were measured at room temperature using a Shimadzu UV-1700 spectrophotometer operating in a wavelength range of 200–1100 nm.

[§] The XPS core-level measurements were performed using a PHI 5000 VersaProbe XPS spectrometer based on a classic X-ray optic scheme with a quartz monochromator and an hemispherical energy analyzer working in the range of binding energies from 0 to 1500 eV. The instrument employed electrostatic focusing and magnetic screening to achieve an energy resolution of $\Delta E \leqslant 0.5$ eV. The pumping of analytical chamber was carried out using an ion pump providing residual pressure better than 10^{-7} Pa. The XPS spectra were recorded using monochromatic AlKα X-ray emission (1486.6 eV); the spot size was 200 μm. To avoid surface contamination, all the samples were freshly cleaved prior to the XPS measurements. The recorded spectra were processed using ULVAC-PHI MultiPak Software 9.8. The XPS background was calculated according to the Shirley method. The calculation error did not exceed 3% for the spectra deconvolution.

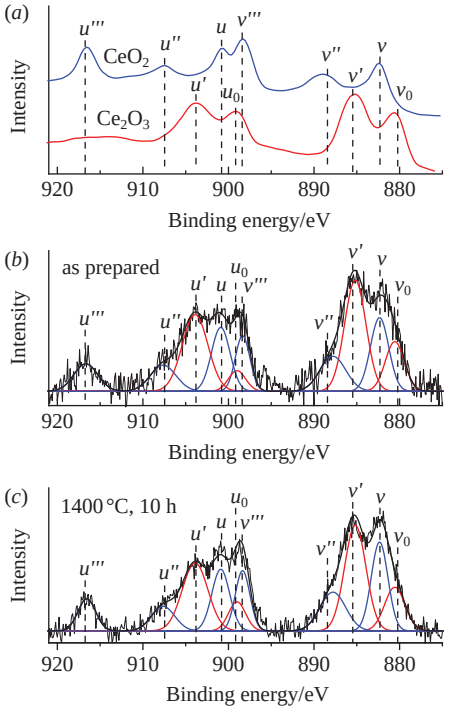

Figure 3 XPS Ce 3*d* spectra of (*a*) reported,[12] (*b*) as prepared and (*c*) annealed Y_2O_3 ceramics.

different positions, wherein O_1 is the lattice oxygen (529.2 eV), O_2 is the absorbed oxygen (531.5 eV), and O_3 corresponds to oxygen defects (530.4 eV).[10,11] The deconvoluted spectra indicate that the high-temperature annealing [see Figure 2(*b*),(*c*)] induces a defect elimination during the oxygen diffusion into the highly defective as prepared ceramics. This effect increases with annealing time, so the defect oxygen content (O_3) has almost completely disappeared in the XPS O 1*s* spectrum of the sample annealed for 10 h [see Figure 2(*c*)].

The XPS Ce 3*d* spectra and the spectra of reference CeO_2 and Ce_2O_3 samples[12] are shown in Figure 3. Let us first to consider the structure of Ce 3*d* spectra of reference compounds Ce_2O_3 and CeO_2. When the 3*d* core level is ionized, the final state is a spin-orbit doublet of $3d_{5/2}$ (with lower binding energy) and $3d_{3/2}$ (with higher binding energy). The structure of each of spin-doublet terms is determined by the electric potential of X-ray 3*d* hole interacting with the excited states, which are attracted by the system for its relaxation after 3*d*-ionization. For Ce^{3+} and Ce^{4+} ions, the initial states are different: f^1 and f^0 states, respectively, so the final states are also different. Each of the spin-doublet terms of Ce^{3+} consists of two lines: v_0 and v' for $3d_{5/2}$ and u_0, u' for $3d_{3/2}$, where v_0 and u_0 correspond to the relaxed final state containing the f^2 configuration and v and u correspond to unrelaxed states with the f^1 configuration coinciding with unexcited (initial) one. In the case of Ce^{4+}, v and u lines correspond to the relaxed final state containing the f^2 configuration, v'' and u'' to partially relaxed state with the f^1 configuration, and v''', u''' to unrelaxed state with the f^0 configuration coinciding with the initial state.[13]

A quantitative analysis of concentration of Ce^{3+} ions based on measured XPS Ce 3*d* spectra can be performed using the formula:[14]

$$[Ce^+] = \frac{A_{v_0} + A_{v'} + A_{u_0} + A_{u'}}{A_{v_0} + A_{v'} + A_{u_0} + A_{u'} + A_v + A_{v''} + A_{v'''} + A_u + A_{u''} + A_{u'''}},$$

where A_i is the integrated area of ith peak.

Using the results of XPS Ce 3*d* spectra deconvolution (see Figure 3), we have performed such an analysis. According to our results, the fraction of Ce^{3+} in Y_2O_3 ceramics doped with

CeO_2 (5 mol%) decreases for the annealed sample (with respect to as prepared one) from 49 to 41%. Note that the question of the oxidation state of cerium ions in oxide materials is quite acute. Special attention is paid to the valence of cerium ions in the optical materials, including yttrium oxide. At the same time, the XPS method allows one not only to establish the presence or absence of Ce^{3+}/Ce^{4+} ions, but also to evaluate their correlation. This approach has already been used in studies of cerium doped yttria;[15] however, in this work, the annealed yttrium oxide powders were investigated, while in our case the initial state of ceramics obtained by vacuum sintering caused a significant effect. The latter has clearly confirmed the presence of Ce^{3+} ions that were not detected previously.[15]

In conclusion, we have revealed a great increase of the optical transparency in the post-annealed Y_2O_3 ceramics doped with CeO_2 (5 mol%) with respect to initial (as sintered) one. The origin of this effect can be attributed to the filling of oxygen vacancies during the high-temperature annealing under air. This is evidenced by the successive decrease in the contribution of defective oxygen to the XPS O 1*s* spectrum during the transition from the freshly sintered sample to the annealed one and also during the increase of annealing time from 1 to 10 h. The cerium ions in annealed samples possess a mixed valence (Ce^{4+} and Ce^{3+}), while a concentration of trivalent cerium is decreasing with the annealing time. This can be used as an additional factor to elevate the amount of bound oxygen in the annealed samples.

This work was supported by the Federal Agency for Scientific Organizations (Theme ‘Electron’, no. AAAA-A18-118020190098-5). The XPS measurements were supported by the Ministry of Education and Science of the Russian Federation (project no. 3.7270.2017/8.9) and the grant from the President of the Russian Federation (grant no. MK-1145.2017.2).

References

1 N. S. Prasad, S. Trivedi, S. Kutcher, C.-C. Wang, J.-C. Kim, U. Hommerich, V. Shukla and R. Sadangi, *Proc. SPIE*, 2009, **7193**, 71931X.
2 M. W. Barsoum, *Fundamentals of Ceramics*, McGraw-Hill, New York, 1997.
3 L. Wen, X. Sun, Z. Xiu, S. Chen and C.-T. Tsai, *J. Eur. Ceram. Soc*., 2004, **24**, 2681.
4 A. Ikesue, I. Furusato and K. Kamata, *J. Am. Ceram. Soc*., 1995, **78**, 225.
5 A. Ikesue and Y. Sato, *J. Ceram. Soc. Jpn*., 2001, **109**, 640.
6 A. Krell, J. Klimke and T. Hutzler, *Opt. Mater*., 2009, **31**, 1144.
7 W. Zhang, T. Lu, N. Wei, B. Ma, F. Li, Z. Lu and J. Qi, *Opt. Mater*., 2012, **34**, 685.
8 L. An, A. Ito and T. Goto, *J. Am. Ceram. Soc*., 2011, **94**, 3851.
9 V. V. Osipov, Yu. A. Kotov, M. G. Ivanov, O. M. Samatov, V. V. Lisenkov, V. V. Platonov, A. M. Murzakaev, A. I. Medvedev and E. I. Azarkevich, *Laser Phys*., 2006, **16**, 116.
10 J. F. Moulder, W. F. Stickle, P. F. Sobol and K. D. Bomben, *Handbook of X-ray Photoelectron Spectroscopy*, ed. J. Chastain, Eden Prairie, MN, 1995.
11 Y. Hu, Z. Li and W. Pan, *RSC Adv*., 2018, **8**, 13200.
12 D. R. Mullins, S. H. Overbury and D. R. Huntley, *Surf. Sci*., 1998, **409**, 307.
13 A. Kotani, T. Jo and J. C. Parlebas, *Adv. Phys*., 1988, **37**, 37.
14 S. Deshpande, S. Patil, S. V. N. T. Kuchibhatla and S. Seal, *Appl. Phys. Lett*., 2005, **87**, 133113.
15 L. Douillard, M. Gautier, N. Thromat, M. Henriot, M. J. Guittet, J. P. Duraud and G. Tourillon, *Phys. Rev. B*, 1994, **49**, 16171.

Received: 9th July 2018; Com. 18/5636